

TIMING AND SPECTRAL STUDIES OF LMC X-4 IN HIGH AND LOW STATES  
WITH *Beppo*-SAX : DETECTION OF PULSATIONS IN THE SOFT SPECTRAL  
COMPONENTS. NAIK<sup>1,2</sup> & B. PAUL<sup>1</sup>*Accepted for Publication in The Astrophysical Journal*

## ABSTRACT

We report here detailed timing and spectral analysis of two *Beppo*-SAX observations of the binary X-ray pulsar LMC X-4 carried out during the low and high states of its 30.5 days long super-orbital period. Timing analysis clearly shows 13.5 s X-ray pulsations in the high state of the super-orbital period which allows us to measure the mid-eclipse time during this observation. Combining this with two other mid-eclipse times derived earlier with the ASCA, we derived a new estimate of the orbital period derivative. Pulse-phase averaged spectroscopy in the high and low states shows that the energy spectrum in the 0.1 – 10 keV band comprises of a hard power-law, a soft excess, and a strong iron emission line. The continuum flux is found to decrease by a factor of  $\sim 60$  in the low state while the decrease in the iron line flux is only by a factor of  $\sim 12$ , suggesting a different site for the production of the line emission. In the low state, we have not found any significant increase in the absorption column density. The X-ray emission is found to come from a very large region, comparable to the size of the companion star. Pulse phase resolved spectroscopy in the high state shows a pulsating nature of the soft spectral component with some phase offset compared to the hard X-rays, as is known in some other binary X-ray pulsars.

*Subject headings:* stars : neutron — Pulsars : individual (LMC X-4) — X-rays : stars

## 1. INTRODUCTION

LMC X-4 is an eclipsing, accretion-powered, binary X-ray pulsar in the Large Magellanic Cloud orbiting around a 20  $M_{\odot}$  O7 III-V companion with an orbital period of  $\sim 1.4$  day (Kelley et al. 1983, Ilovaisky et al. 1984) and pulse period of  $\sim 13.5$  s (White 1978, Li, Rappaport & Epstein 1978, Lang et al. 1981). X-ray eclipses with a 1<sup>d</sup>.4 recurring period were discovered by Li et al. (1978) and White (1978). X-ray pulsations with a period of 13.5 s were first detected in LMC X-4 from *SAS 3* observations in 1976 and 1977 only during the infrequent flaring events by Kelley et al. (1983), who also derived the orbital solution from pulse arrival delay measurements. During a high state in 1983, *EXOSAT* observations detected the pulsations both during flaring and non-

flaring episodes (Pietsch et al. 1985). Using subsequent pulse timing measurements with *GINGA*, *ROSAT* (Levine et al. 1991, Woo et al. 1996) and RXTE (Levine et al. 2000), an orbital period decay with a time scale of  $\sim 10^6$  yr<sup>-1</sup> was measured, which is similar to the period decay rate in other high mass accreting binary pulsars (Cen X-3, SMC X-1 etc.).

Analogous to the well known X-ray pulsar Her X-1, LMC X-4 exhibits a periodic long term intensity variation at 30.5 day (Lang et al. 1981). The super-orbital period has recently been found to be decreasing (Paul & Kitamoto 2002). In the case of LMC X-4, the X-ray flux varies by two orders of magnitude between the high and low intensity states of the super-orbital period. Varying obscuration by the accretion disk due to precession provides a good explanation for the long term

<sup>1</sup>Tata Institute of Fundamental Research, Homi Bhabha Road, Mumbai 400 005, India  
sachi@tifr.res.in, bpaul@tifr.res.in

<sup>2</sup>Department of Physics, University College Cork, Cork, Ireland  
sachi@ucc.ie

periodic intensity variations. The 13.5 s X-ray pulsation is not yet detected during the low state of the super-orbital period indicating that most of the radiation observed in low state is probably reprocessed emission from the stellar wind of the companion star. The X-ray spectrum during eclipse of the neutron star, which consists only of scattered/reflected radiation was found to be nearly identical in shape and strength throughout the super-orbital period, supporting the disk obscuration hypothesis (Woo et al. 1995). However, observations with the *RXTE* (Heindl et al. 1999) did not detect any significant change in the absorption column density in different phases of the super-orbital period. One possibility that was pointed out is that in low state, part of the X-ray emission from the central source is completely blocked by the disk and the rest is observed with the Galactic absorption. It should be noted that, for sensitive measurements of absorption column density, observations with good soft X-ray spectral capability are required.

The X-ray spectrum of LMC X-4 consists of, in addition to a hard power-law component, a soft excess below 1 keV and an iron emission line at 6.4 keV (Woo et al. 1996). Iron K shell emission lines in X-ray pulsars are usually narrow, but the equivalent width can sometimes be as large as  $\sim 1$  keV or more. These lines are produced by illumination of neutral or partially ionized material in accretion disk, stellar wind of high mass companion star, material in the form of circumstellar shell, material in the line of sight, or accretion column. Expectedly, the iron emission line parameters are often found to be correlated to the continuum hard X-ray flux, absorption column density etc. Using a large number of *RXTE*/*PCA* observations of LMC X-4 made in different phases of the super-orbital period, a correlation was found between the line flux and the continuum flux, along with highly variable nature of the equivalent width of the line during low state (Naik & Paul 2003).

It is known that X-ray pulsars those do not suffer from strong absorption by material in the line of sight show presence of soft X-ray excess above the extrapolated hard power-law component (Paul et al. 2002, and references therein). In some pulsars, the soft excess is also found to pulsate, often with a phase difference with respect to the hard component. Origin of the pulsating soft component is not yet understood clearly, at

least for the bright pulsars in LMC and SMC. In LMC X-4, a small Galactic absorption column density and lack of local absorbing material allows us to probe the soft X-ray emission with some detail. Observations of LMC X-4 with *ASCA* detected the soft excess but were found to be inconclusive regarding the nature of the soft component (Paul et al. 2002). The latter is due to a small pulse fraction of this pulsar and also to the fact that the *ASCA* spectrometers are not sensitive at energies where the soft excess dominates the power-law component in LMC X-4.

We have carried out detailed timing and spectral analysis of two observations of LMC X-4 with the narrow field instruments of *Beppo-SAX* during one high and one low intensity states of LMC X-4. We aimed to detect pulsations in the *Beppo-SAX* observation carried out in the high state and to determine the mid-eclipse time during this observation. From pulse phase averaged spectral studies in the two states, we investigate relations of the iron line parameters with the continuum flux. To investigate the nature of the soft excess, pulse-phase-resolved spectral analysis has been carried out for the high state observation. In the subsequent sections we give details of the observations, the results obtained from the timing and spectral analysis, followed by a discussion on the results obtained from these two *Beppo-SAX* observations.

## 2. OBSERVATIONS

The 2–12 keV X-ray light curve of LMC X-4 taken with the *RXTE-ASM* for last six years, is shown in Figure 1, folded at the present super-orbital period of 30.276 days (Paul & Kitamoto 2002). Two observations of LMC X-4 were made with the *Beppo-SAX* narrow field instruments during 1997 March 13 10:48 to March 15 08:17 (UT) and 1998 October 20 22:39 to October 22 08:05 (UT) in the low and high states of the source respectively. The durations of these two observations with respect to the phase of the long period are also shown in Figure 1. We have used archival data from these two observations in the present work.

For the present study, we have used data from the Low and Medium Energy Concentrator Spectrometers *LECS* and *MECS* and the Phoswich Detector System *PDS* on-board *Beppo-SAX* satellite. In the 1997 observation, the hard X-ray instrument *PDS* with a larger field of view con-

tained mostly photons from a nearby transient source EXO 053109–6609.2, which is only 0.5 degree away from LMC X-4 (Burderi et al. 1998). The broad band spectrum (0.1–100 keV) from the 1998 Beppo-SAX observation has been reported by La Barbera et al. (2001). To obtain energy resolved pulse profiles in hard X-rays, we have used PDS data from the 1998 observation.

The MECS consists of two grazing incidence telescopes with imaging gas scintillation proportional counters in their focal planes. The LECS uses an identical concentrator system as the MECS, but utilizes an ultra-thin entrance window and a drift less configuration to extend the low-energy response to 0.1 keV. Time resolution of the instruments during these observations was 15.25  $\mu$ s and energy resolutions of LECS and MECS are 25% at 0.6 keV and 8% at 6 keV respectively. The PDS consists of a square array of four independent NaI(Tl)/CsI(Na) phoswich scintillation detectors. The energy resolution of PDS instrument is 15% at 60 keV. The time resolution of the PDS instruments during 1998 observation was 0.25 ms. For a detailed description of the Beppo-SAX mission, we refer to Boella et al. (1997).

### 3. TIMING ANALYSIS

The light curves of LMC X-4 during these two *Beppo-SAX* observations obtained with the LECS and MECS detectors are shown in Figure 2 with respect to the orbital phase (mid-eclipse time = orbital phase 0.5). During the 1997 observation, which was in a low state, a smooth intensity variation is observed throughout the orbital period and the eclipse is not clearly seen. Near the end of the low state observation, an increase in count rate is noticed which is similar to the flares observed earlier in the low state with *ROSAT* (Woo et al. 1995). Similar to the other high state observations of LMC X-4, the 1998 observation clearly shows an eclipse during which the X-ray intensity decreases sharply to a very low level.

For timing analysis, the arrival times of the photons were first converted to the same at the solar system barycenter. Light curves with time resolution of 0.25 s were extracted from circular regions of radius 4' around the source. The pulses from LMC X-4 loose coherence within a relatively short time scale of few thousand seconds due to a short orbital period of 1.4 days while the semi-amplitude of the arrival time delay due to orbital motion is 26.3 s. Additionally, the relatively

small effective area of the Beppo-SAX telescopes and small pulse fraction of LMC X-4 makes it difficult to detect pulse arrival times from small segments of the light curve. Therefore, to detect the pulsations and also the mid-eclipse times during these observations, we have first corrected the light curve for the binary motion. The orbital parameters, namely the semi-amplitude was taken to be 26.31 s and the mid-eclipse time was derived from the quadratic solution given by Levine et al. (2000). The binary arrival time delay correction was applied with a range of trial mid-eclipse times around the value extrapolated from Levine et al. (2000). Pulse folding and  $\chi^2$  maximization method was applied to all the corrected light curves. The distribution of maximum  $\chi^2$  against the trial mid-eclipse times obtained from each pulse folding analysis is shown in Figure 3 for the high state observation in 1998. The maximum  $\chi^2$  distribution has a Gaussian profile around the expected value of the mid-eclipse time, the center of which gives the correct value. Using the same method we did not detect any pulsations in the low state. The result of the pulse folding analysis corresponding to the peak of the curve in Figure 3 is shown in Figure 4, which clearly shows the detection of pulsations in this observation contrary to La Barbera et al. (2001). In the high state, the pulsations were in fact detected independently in light curves of the LECS, MECS and PDS detectors. The pulse profiles obtained from the high state light curves of the LECS, MECS, and PDS in different energy bands are shown in Figure 5. From this analysis, we have derived the pulse period of LMC X-4 to be 13.50260(12) s and the mid-eclipse time MJD 51106.6399(25) corresponding to orbit number 5877.

Combining the new determination of mid-eclipse time with the previous measurements (Levine et al. 2000 and references therein, Paul et al. 2002) we fitted a second-order polynomial to derive the orbital decay rate. Residuals of the orbital mid-eclipse time history of LMC X-4 relative to a constant period are shown in Figure 6. The solid line in the figure shows the quadratic nature of the mid-eclipse time history. We derive a period decay rate of  $\frac{\dot{P}_{\text{orb}}}{P_{\text{orb}}} = (9.89 \pm 0.05) \times 10^{-7} \text{ yr}^{-1}$ .

The pulse profiles in different energy bands are shown in Figure 5. In the low energy band (0.1–1.0 keV of LECS, top panel), it is nearly sinusoidal

and has a complex structure in the energy band of 4.0–10.0 keV (MECS, bottom panel) with multiple dips superposed on a smooth sinusoidal profile. A phase difference between the sinusoidal pulse components of the two energy bands is also visible in the figure. At intermediate energies (1.0–4.0 keV, both LECS and MECS), the pulse profile is a mixture of the above two. The pulse fraction is less than 10% and these features are similar to the known pulsation properties of LMC X-4. Though the pulsations are seen in the PDS light curves in 15.0–60 keV energy band (top-right three panels of Figure 5), the pulse profiles do not show the complex dipping feature, as seen in the MECS profiles, and are similar to those obtained from the LECS light curves with certain phase difference. The light curve above 60 keV is mainly background dominated and we did not detect pulsations in the 60–200 keV range. The transient X-ray pulsar EXO 0531-66 which has a pulse period of 13.7 s, close to that of LMC X-4 was in the field of view of the PDS instrument. This source was detected in the LECS and MECS instruments at an intensity level of about 0.2% of LMC X-4. From a period search of the PDS light curve in a range covering the pulse period of both LMC X-4 and EXO 0531-66, we have verified that contamination of the PDS folded light curve of LCM X-4 was minimal.

#### 4. PULSE PHASE AVERAGED SPECTROSCOPY

For spectral analysis, we have extracted LECS spectra from regions of radius  $6'$  centered on the object (the object was at the center of the field of view of both the instruments). The combined MECS source counts (MECS 1+2+3 in the 1997 observation and MECS 2+3 in the 1998 observation) were extracted from circular regions with a  $4'$  radius. For spectral fitting, the September 1997 LECS and MECS1 response matrices were used. Background spectra for both LECS and MECS instruments were extracted from appropriate source-free regions of the field of view with extraction region on the detector similar to the source extraction regions. Some rebinning was done to allow the use of  $\chi^2$ -statistic. Events were selected in the energy ranges 0.1–4.0 keV for LECS and 1.65–10.0 keV for MECS where the instrument responses are well determined. Combined spectra from the LECS and MECS detectors, after appropriate background subtraction, were fitted simultaneously. All the spectral pa-

rameters, other than the relative normalization, were tied to be the same for both detectors and the minimum value of hydrogen column density  $N_H$  was set at the value of Galactic column density in the source direction.

#### 4.1. Low state

In the low state observation of 1997, the source count rate is about two orders of magnitude lower than the high state. Therefore, spectral fitting required significant rebinning. The spectrum, when fitted to a single power-law model with line of sight absorption, showed significant soft excess below 1 keV. Addition of a soft component in the model improves the spectral fit; we have tried two different components such as black-body emission and bremsstrahlung component to fit the soft excess. Results of the spectral fits are given in Table 1. From the spectral fitting, we are unable to distinguish between these two models of the soft component. The low state photon spectrum along with a spectral model comprising of three components, a hard power-law, a Gaussian emission line and a bremsstrahlung emission are shown in Figure 7. Two notable features of the low state spectrum are that the power-law component is very hard with a photon index of  $\sim 0.1$ , and the iron line equivalent width is large,  $\sim 1.3$  keV. Both of these have been observed earlier with the RXTE (Naik & Paul 2003). The line of sight absorption during low intensity state is found to be  $\sim 5 \times 10^{20}$  atoms  $\text{cm}^{-2}$ , similar to the Galactic column density, and the characteristic temperature of the soft component is lower than that in the high state.

#### 4.2. High state

A power-law fit to the high state spectrum shows a large soft X-ray excess. Similar to the low state, we tried to fit the soft excess with different single components : black-body, thermal bremsstrahlung and soft power-law, none gives a satisfactory fit. Finally we found that a combination of any two of these components for the soft excess improves the spectral fit to some extent. The best-fit model is the one comprising a hard power-law of photon index 0.65, an iron  $K_\alpha$  emission line of equivalent width 240 eV, a black-body component of temperature 0.15 keV and a soft power-law with photon index  $\sim 3$ . The LECS and MECS count rate spectra are shown in Figure 8 along with contributions of individual

components. Irrespective of the model chosen to fit the soft excess, the soft component starts dominating the spectrum at energies below 0.8 keV.

## 5. PULSE PHASE RESOLVED SPECTROSCOPY

Since we have not detected any pulsations in the low state observation of 1997, the pulse phase resolved spectroscopy is done only on the 1998 data set to understand the nature of the soft component. The photon arrival times in the LECS and MECS event files were corrected for the solar system barycenter and for the arrival time delays due to orbital motion. Following this, spectra were accumulated into 16 pulse phases by applying phase filtering in the FTOOLS task XSELECT. As in the case of phase-averaged spectroscopy, the background spectra were extracted from source free regions in the event files and appropriate response files were used for the spectral fitting.

Each pulse phase resolved spectra has much inferior signal to noise ratio compared to the phase averaged spectrum. Therefore, sometimes it is not possible to constrain all the model parameters, specially if a complicated spectral model is used. Since our aim is to investigate nature of the soft excess (whether pulsating or not) we used only two models, in which a single component (either a soft power-law or a bremsstrahlung) is used for the soft excess and a relatively low reduced  $\chi^2$  is obtained. For the phase resolved spectra, the iron-line energy, line-width and  $N_H$  were fixed to their phase-averaged values and all the other spectral parameters were allowed to vary. The continuum flux and the fluxes of the soft and hard components in 0.1 – 10.0 keV energy range were estimated for all the 16 phase-resolved spectra. The modulation in the X-ray flux for the hard and soft spectral components and the total flux are shown in Figure 9 along with the  $1\sigma$  error estimates. Pulse phase resolved spectral analysis shows that modulation of the hard power-law flux is very similar to the pulse profile at higher energies. A pulsating nature of the soft-spectral component is clearly detected irrespective of the spectral model used. The pulsating soft component has a nearly sinusoidal profile, dissimilar to the complex profile seen at higher energies, with a certain phase difference with the hard component. These properties are very similar to what is seen in Her X-1 (Endo et al. 2000) and SMC X-1 (Paul et al. 2002).

## 6. DISCUSSION

### 6.1. *Orbital evolution*

There are several ways to measure orbital ephemeris of X-ray binaries from X-ray observations. Pulse frequency modulation or arrival time delay measurement of X-ray pulsars gives very accurate measurement of mid-eclipse time ( $T_{\frac{\pi}{2}}$ ) of binary X-ray pulsars and has so far been used to measure the orbital parameters of a large number of binary X-ray pulsars. A quadratic nature of the mid-eclipse time history during the last two/three decades unambiguously established an orbital evolution with a time scale of about  $10^5 - 10^6$  yr in several binary X-ray pulsars (Cen X-3, Nagase et al. 1992; LMC X-4, Levine et al. 2000; SMC X-1, Wojdowski et al. 1998 etc.). In case of low mass X-ray binary pulsars, the orbital evolution is mainly due to conservative mass transfer from the companion to the neutron star whereas in case of high mass X-ray binaries, it is either due to mass loss from the system and/or strong tidal interaction between the two stars. The measurement of one new mid-eclipse times of LMC X-4 with *Beppo-SAX* and two with *ASCA* (Paul et al. 2002) allows us to determine the orbital period derivative of the source with better accuracy. It has been pointed out before that tidal interaction is probably the dominating effect in orbital evolution of LMC X-4 (Levine et al. 2000).

### 6.2. *The iron emission line*

Spectral analysis of the high and low states of LMC X-4 showed significant differences. Presence of a prominent iron emission line can be seen in the low intensity state of the source (Figure 7). While the continuum flux in 0.1–10 keV band in the two states differ by a factor of  $\sim 60$ , the iron line flux differs only by a factor of  $\sim 12$ . This results in a much larger equivalent width of 1.26 keV in the low state compared to 200 eV in the high state. In view of an obscuring precessing accretion disk model for the super-orbital period, it is interesting to note that the column density is very similar in the two states and are close to the Galactic value. It was suggested (Heindl et al. 1999) that if the low state X-rays are due to Compton scattering by circumstellar material, significant obscuration by the accretion disk in the low state may still be true. Partial coverage of the

TABLE 1  
SPECTRAL PARAMETERS FOR LMC X-4 DURING LOW INTENSITY STATE

Parameter	Model-I	Model-II	Model-III
$N_H$ <sup>1</sup>	5.5	5.5 <sup>+4.9</sup>	5.5 <sup>+3.0</sup>
$\Gamma$	0.11	0.06 <sup>+0.07</sup> <sub>-0.1</sub>	0.11±0.06
$kT$ (keV)	—	—	0.14±0.02
$kT_{Br}$ (keV)	—	0.4 <sup>+0.11</sup> <sub>-0.09</sub>	—
$Fe_E$ (keV) <sup>2</sup>	6.45	6.46±0.05	6.45 <sup>+0.07</sup> <sub>-0.04</sub>
$Fe_W$ (keV) <sup>3</sup>	0.26	0.26±0.08	0.26±0.07
$W_0$ (keV) <sup>4</sup>	1.26	1.26	1.26
Model flux <sup>5</sup>	2.8	3.1	3.3
Fe line flux <sup>5</sup>	0.39	0.37	0.39
Reduced $\chi^2$	2.8 (29)	1.17 (27)	1.36 (27)

<sup>1</sup> :  $10^{20}$  atoms  $\text{cm}^{-2}$ , <sup>2</sup> : Iron line energy, <sup>3</sup> : Iron line width, <sup>4</sup> : Iron equivalent width, <sup>5</sup> :  $10^{-12}$  ergs  $\text{cm}^{-2} \text{s}^{-1}$

Model-I =  $W_{abs} * (\text{Po} + \text{Gau})$ , Model-II =  $W_{abs} * (\text{Br} + \text{Po} + \text{Gau})$ , Model-III =  $W_{abs} * (\text{BB} + \text{Po} + \text{Gau})$

$W_{abs}$  = Photoelectric absorption parameterized as equivalent hydrogen column density  $N_H$ , Po = Power-law with photon index  $\Gamma$ , BB = blackbody component with temperature  $kT$ , Br = thermal-bremsstrahlung-type component with plasma temperature  $kT_{Br}$  and Gau = Gaussian function for iron  $K_\alpha$  line.

hard X-ray emission could be a possible explanation for the low state. However, we found that addition of a partial covering model component to the hard power-law does not fit the low state spectrum.

The spectral results obtained from present work are consistent with those obtained from the *RXTE*-PCA observations (Naik & Paul 2003). However, a much better sensitivity for weak sources and better energy resolution of *BeppoSAX* LECS and MECS compared to *RXTE*-PCA instruments gives improved confidence in the equivalent width measurements of the iron emission line. A smaller iron line flux in the low state indicates that most of the line emission is produced in a region comparable to or smaller than the size of the obscuring material, probably the accretion disk. But an increased equivalent width of the iron line in low state also indicates that a part of the emission line must originate in a region further away from the neutron star. It is known that the HMXB pulsars often show several iron line components from different ionization species, probably produced in different regions of the system. The best example is the case of Cen X-3 where at least three components with different variability characteristics were resolved (Ebisawa et al. 1996). The flux evolution of different line components during eclipse egress suggests that the 6.4 keV line is emitted close to the neutron star, while the other components are probably emitted in a more extended highly ionized plasma (Nagase et al. 1992, Ebisawa et al. 1996). In the case of LMC X-4 also, La Barbera et al. (2001) claimed detection of more than one component with one of them being at 6.1 keV. High spectral resolution observations with *Chandra* or future *ASTRO-E* mission will allow one to find out whether these two species of iron have different ionization state. High spectral resolution observations in different phases of the super-orbital and orbital periods of LMC X-4, including during the eclipse, will finally help to settle the issue regarding the origin of the iron emission line in LMC X-4.

### 6.3. Pulsations of the soft excess and its origin

A soft excess above the hard power-law component is now known to be present in several accreting pulsars and the soft component is also known to be pulsating in some of these sources. The soft excess has been modeled with several differ-

ent types of emission, but no single model is applicable to all sources with soft excess. A black-body type pulsating soft excess can describe the emission from Her X-1 well (Endo et al. 2000), however, it runs into problem in case of the more luminous sources like SMC X-1 and LMC X-4 (Paul et al. 2002). In some sources, a bremsstrahlung type of soft emission describes the spectrum well. However, since the emission region has to be very large and the cooling time scale is also very large, such an emission is not expected to pulsate. The soft excess in LMC X-4 is more complex and more than one component is needed to model the soft excess. However, when a bremsstrahlung component is included, it produces most of the soft excess and the pulsating soft excess requires this component to pulsate. LMC X-4 has a very small pulse fraction, and the soft excess peaks at energies lower than the *ASCA* threshold. As a result, *ASCA* observations of LMC X-4 were inconclusive regarding the pulsations of the soft excess in LMC X-4. In the present work with *BeppoSAX*, we have obtained definite detection of pulsations in the soft excess irrespective of the spectral model used.

In the low state, the LECS and MECS light curves (Figure 2) show large amplitude but gradual intensity variation over the entire binary orbit. The sharp eclipse, that is easily detectable in the high state, is not clear in the low state at all. This indicates that in low state, the observed X-rays are due to reprocessing from a scattering region that has size comparable to that of the companion star. It is possible that in different orbital phases part of the scattering region is blocked from view by the companion star. The amplitude of variation, i.e., ratio between the maximum and minimum in the low state binary light curve is larger in MECS compared to LECS. This is possible if the soft excess is produced in a larger region and the hard power-law component originated near the neutron star is heavily absorbed with the absorption highly varying with orbital phase. Using a radius of  $8.1 R_{\odot}$  of the companion star (Woo 1993) and a binary separation of 26.31 lt-s (Levine et al. 1991), the solid angle subtended by the companion star at the neutron star is calculated to be  $\sim 4\pi/7$ . In the present work, the soft excess flux in the low and high states of LMC X-4 are measured to be about about 18% of the hard power-law flux. Therefore, one probable site for production of the soft excess is the surface of the

companion star, which can work as a reprocessing agent. Different visibility of the stellar surface that is irradiated by the neutron star can cause the observed orbital soft X-ray intensity modulation in the low state.

#### ACKNOWLEDGMENTS

We thank the referee for her/his valuable suggestions that helped us to improve the content

of this paper and also regarding analysis of the PDS data. We thank A. R. Rao for some valuable discussions. The Beppo-SAX satellite is a joint Italian and Dutch program. We thank the staff members of Beppo-SAX Science Data Center and RXTE/ASM group for making the data public.

#### REFERENCES

- Boella, G., Butler, R. C., Perola, G. C., Piro, L., Scarsi, L., Bleeker, J. A. M. 1997, *A&AS*, 122, 299
- Boroson, B., Kallman, T., McCray, R., Vrtillek, S. D., & Raymond, J. 1999, *ApJ*, 519, 191
- Burderi, L., di Salvo, T., Robba, N. R., del Sordo, S., Santangelo, A., & Segreto, A. 1998, *ApJ*, 498, 831
- Endo, T. 2000, Ph. D. thesis
- Endo, T., Nagase, F., & Mihara, T. 2000, *PASJ*, 52, 223
- Heindl, W. A., Gruber, D. E., Rothschild, R. E., Crannell, C. J., Lang, F. L., Kaplan, L. 1999, American Astronomical Society, HEAD meeting 31, 15.21
- Ilovaisky, S. A., Chevalier, C., Motch, C., Pakull, M., van Paradijs, J., & Lub, J. 1984, *A&A*, 140, 251
- Katz, J. I. 1973, *NPhS*, 246, 87
- Kelley, R. L., Jernigan, J. G., Levine, A., Petro, L. D., & Rappaport, S. 1983, *ApJ*, 264, 568
- Kohno, M., Yokogawa, Jun, & Koyama, K 2000, *PASJ*, 52, 299
- Lang, F. L. et al. 1981, *ApJ*, 246, L21
- Leahy, D. A. 2001, *ApJ*, 547, 449
- Levine, A., Rappaport, S., Putney, A., Corbet, R., & Nagase, F. 1991, *ApJ*, 381, 101
- Levine, A. M., Rappaport, S. A., & Zojcheski, G. 2000, *ApJ*, 541, 194
- Li, F., Rappaport, S., & Epstein, A. 1978, *Nature*, 271, 37
- Nagase, F., Corbet, R. H. D., Day, C. S. R., Inoue, H., Takeshima, T., Yoshida, K., & Mihara, T. 1992, *ApJ*, 396, 147
- Nagase, F., Hayakawa, S., Sato, N., et al. 1986, *PASJ*, 38, 547
- Naik, S., & Paul, B. 2003, *A&A*, 401, 265
- Paul, B., & Kitamoto, S. 2002, *JApA*, 22, 33
- Paul, B., Nagase, F., Endo, T., Dotani, T., Yokogawa, J., & Nishiuchi, M. 2002, *ApJ*, 579, 411
- Pietsch, W., Voges, W., Pakull, M., & Staubert, R. 1985, *SSRv*, 40, 371
- Roberts, M. S. 1974, *Sci*, 183, 371
- Vrtillek, S. D., Boroson, B., Cheng, F. H., McCray, R., & Nagase, F. 1997, *ApJ*, 490, 377
- Yokogawa, J., Paul, B., Ozaki, M., Nagase, F., Chakrabarty, D., Takeshima, T. 2000, *ApJ*, 539, 191
- White, N. E. 1978, *Natur*, 271, 38
- Wojdowski, P., Clark, G. W., Levine, A. M., Woo, J. W., & Zhang, S. N., 1998, *ApJ*, 502, 253
- Woo, J. W. 1993, *PhDT*, 26
- Woo, J. W., Clark, G. W., & Levine, A. M. 1995, *ApJ*, 449, 880
- Woo, J. W., Clark, G. W., Levine, A. M., Corbet, R. H. D., & Nagase, F. 1996, *ApJ*, 467, 811



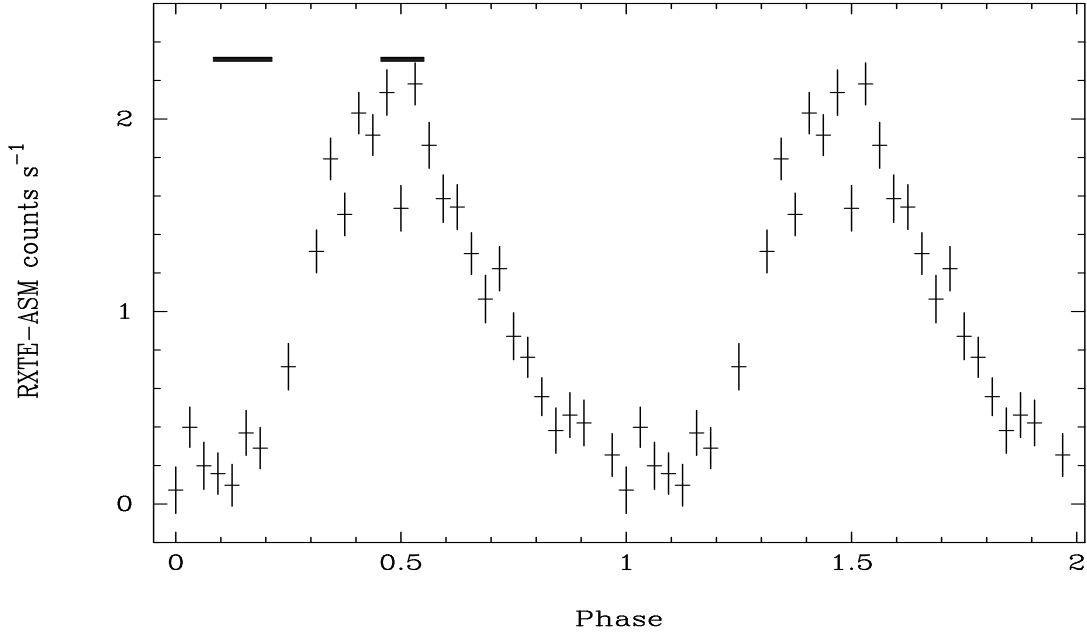


FIG. 1.— The RXTE-ASM light curve of LMC X-4, in 2–12 keV energy range, folded at the long term period of  $30.276 \pm 0.009$  days. The durations of the *Beppo-SAX* observations with respect to the phase of the long period are marked at the top with bold lines.

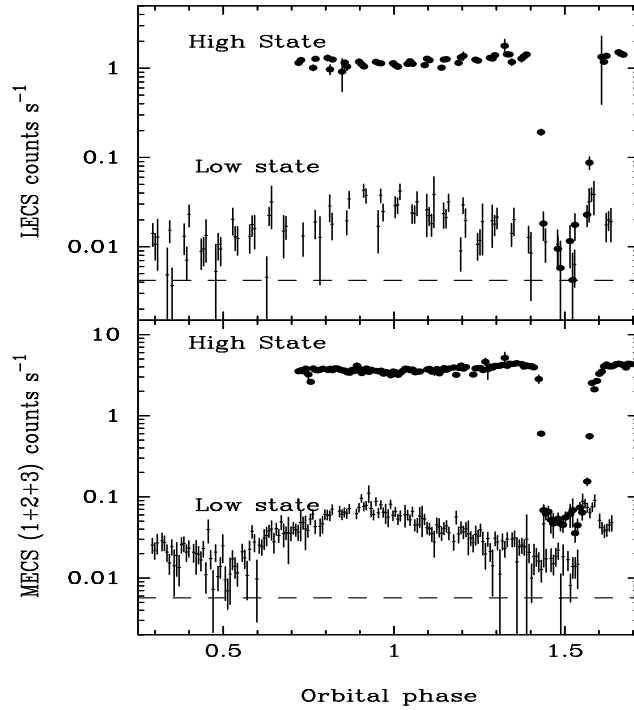


FIG. 2.— The LECS and MECS light curves, in 0.1–10 keV and 1.3–10.0 keV energy ranges respectively, from the two *Beppo-SAX* observations in low and high states. The X-axis represents the orbital phase with mid-eclipse occurring at phase 0.5 and 1.5. The background count rates, measured from blank sky observations are shown with dashed lines. The MECS high state observation was made with only 2 of the 3 detectors and the count rate has been normalized to 3 detectors.

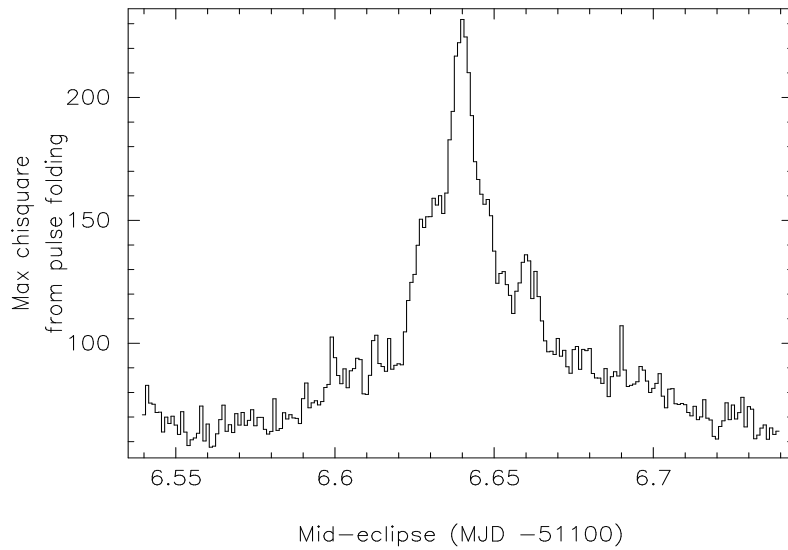


FIG. 3.— The maximum  $\chi^2$  obtained from pulse folding technique is plotted here against the trial mid-eclipse epochs for the 1998 *Beppo-SAX* observation of LMC X-4.

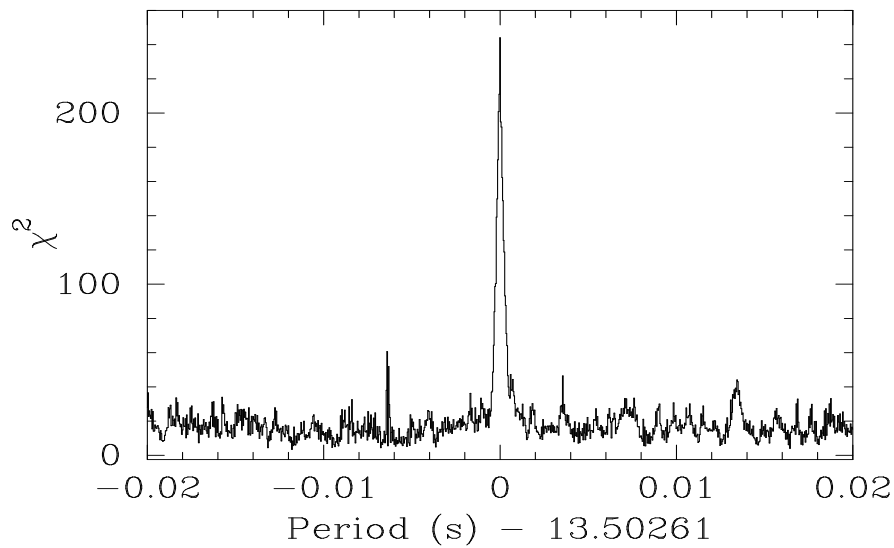


FIG. 4.— Result of the epoch folding test on the high state MECS light curve of LMC X-4.

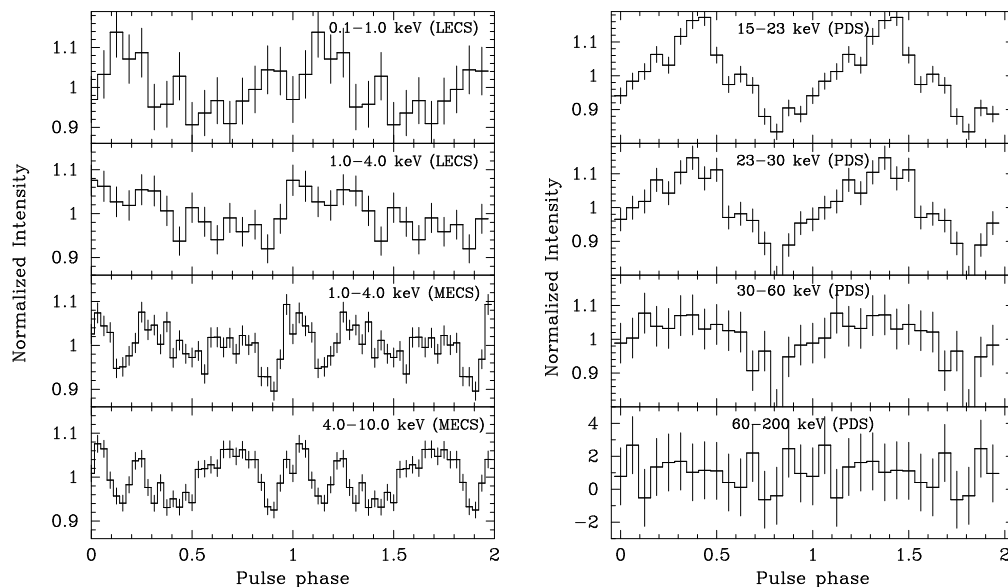


FIG. 5.— LECS and MECS pulse profiles of LMC X-4 in the high state are shown here in the left panels for different energy bands with 16 and 32 phase bins per pulse respectively. Energy resolved pulse profiles from the PDS are shown in the right panels. Two pulses are shown for clarity.

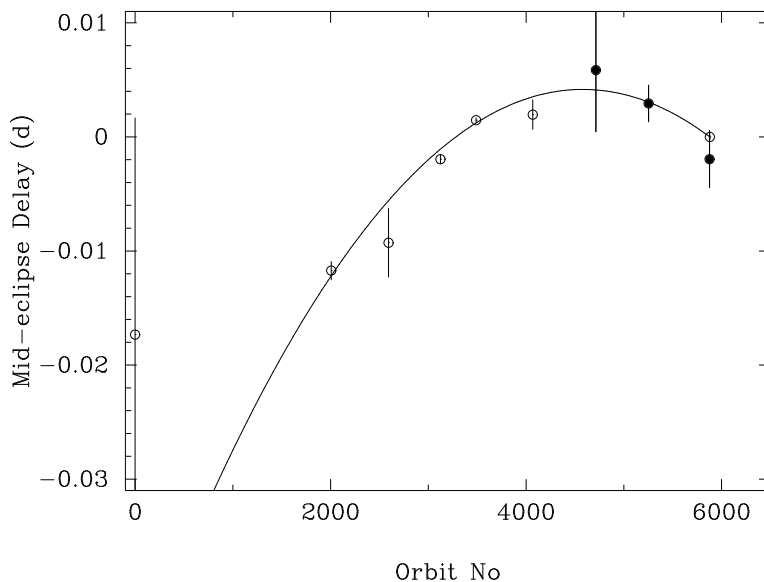


FIG. 6.— The residual orbital epochs of LMC X-4 relative to a constant orbital period  $P = 1.40839374$  d. The new measurements, after Levine et al. 2000, are shown as filled circles. The best-fit quadratic function to the residuals is shown as a curve.

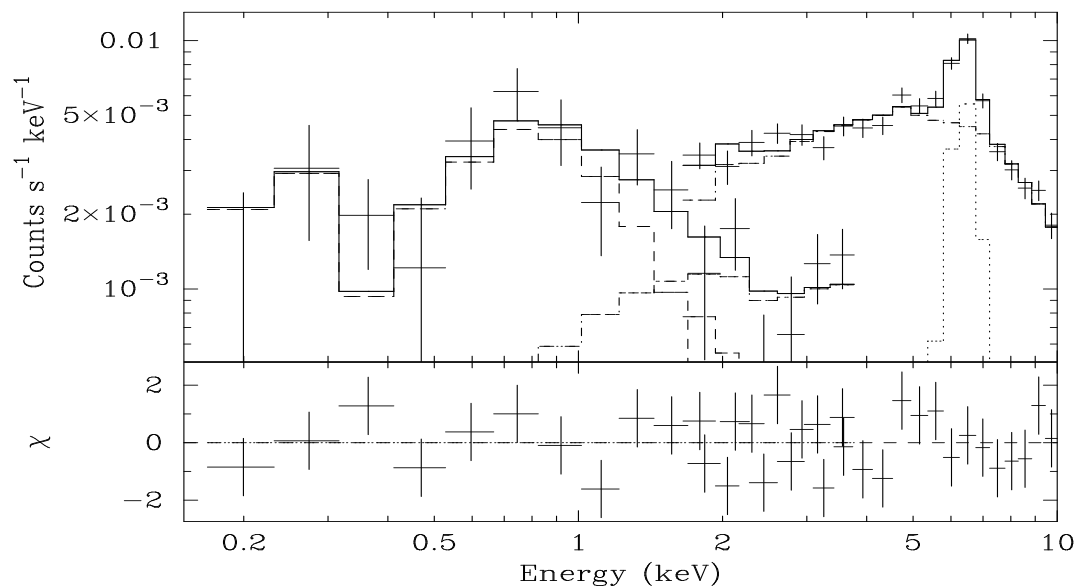


FIG. 7.— The low state LECS and MECS count rate energy spectra in 0.1–10 keV energy band with the folded model comprising of a thermal-bremsstrahlung, a hard power-law component and a broad iron emission line are shown here. The bottom panel shows the contributions of the residuals to the  $\chi^2$  for each energy bin.

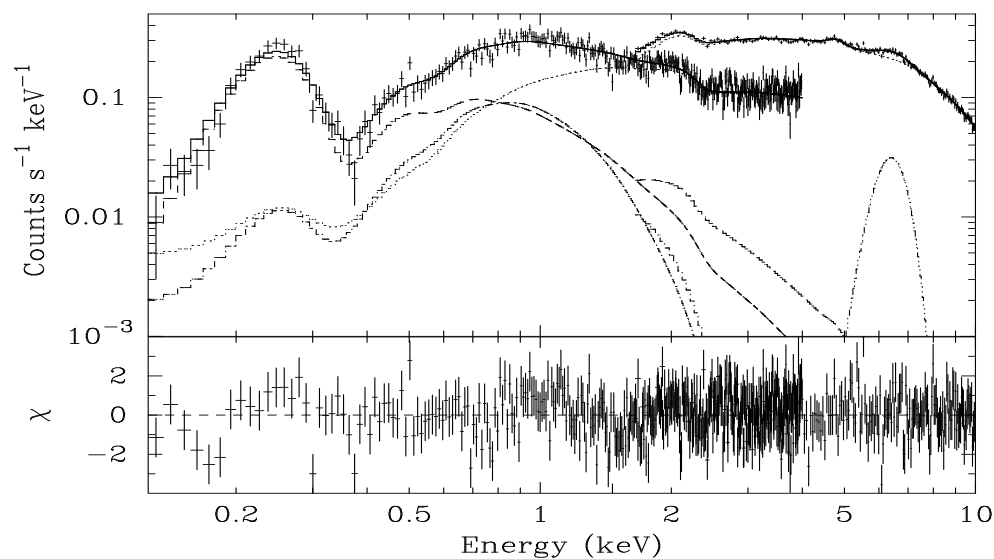


FIG. 8.— High intensity state energy spectra of LMC X-4 obtained with the LECS and MECS detectors, along with the best-fit model comprising a hard power law component, a broad iron emission line, a soft blackbody emission, and a soft power law. The bottom panel shows the contributions of the residuals to the  $\chi^2$  for each energy bin.

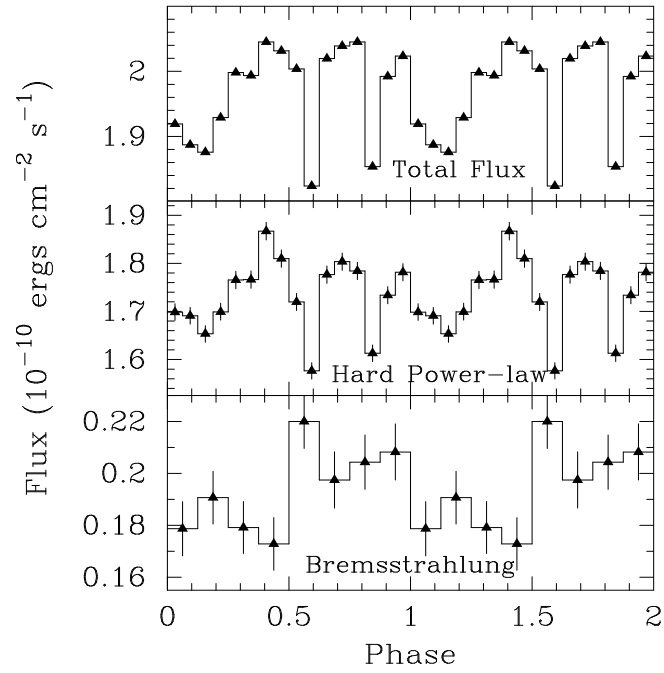


FIG. 9.— Modulation of the total flux, hard power-law flux and flux of the soft spectral component in 0.1 – 10.0 keV energy band of LMC X-4 obtained from the pulse-phase-resolved spectroscopy of the LECS and MECS spectra during the high intensity state of the super-orbital period. The lower panel is rebinned to 8 bins per pulse for clear visibility of the pulsations in the soft component.